Journal of Fluorescence
https://doi.org/10.1007/s10895-020-02651-7

ORIGINAL ARTICLE

A Simple Isoniazid-Based N-Acylhydrazone Derivative as Potential Fluorogenic Probe for Zn^{2+} Ions

Daniela Corrêa Santos [1,2] · Paulo José Sousa Maia [1] · Marcos Antonio de Abreu Lopes Jr. [1,3] · Josué Sebastián Bello Forero [3] · Andréa Luzia Ferreira de Souza [1,3]

Received: 14 July 2020 / Accepted: 9 November 2020

Abstract

This study evaluated three isoniazid-based *N*-acylhydrazone derivatives (**HL1**, **HL2**, and **HL3)** varying their substituting groups (-H, -$N(CH_3)_2$, and -NO_2) as potential chemosensors for Zn^{2+} ions. To this end, the absorption and emission properties of these derivatives were investigated in the presence of Zn^{2+} ions. Results point to the derivative **HL2** as the best chemosensor for Zn^{2+} ions because of its comparatively higher sensitivity. The color of this derivative changed from colorless to strong yellow with zinc addition, as indicated by the shift in UV-vis spectrum. Moreover, **HL2** was the only derivative to emit fluorescence in the presence of Zn^{2+} ions, attributable to PET inhibition and bond isomerization promoted by coordination with this metal. LOD, LOQ, and binding constant values for **HL2** + Zn^{2+} were 0.43 μmol.l^{-1}, 0.93 μmol.l^{-1}, and 5.04×10^{12} l.mol^{-1}, respectively. The fluorescence of **HL2** with other metal ions (Fe^{3+}, Mg^{2+}, Na^{+}, Cd^{2+}, Cu^{2+}, Co^{2+}, Ni^{2+}, Ca^{2+}, and K^{+}) was also investigated. Zn^{2+} yielded the best result without Cd^{2+} interferences. *Job's Plot* showed that the stoichiometric ratio of the complex formed by **HL2** and Zn^{2+} ions is 2:1 (ligand:metal). The strip test with adsorbed **HL2** indicated fluorescence in the presence of zinc ions under 365 nm UV irradiation.

Keywords Zinc(II) · Fluorescence · *N*-acylhydrazone · Isoniazid · Chemosensor

Introduction

Zinc is the second most abundant transition metal in the human body; it is directly involved in many physiological and pathological processes in living organisms [1]. Zn^{2+} ions are key elements in structural components of numerous proteins and act as catalysts in enzymes central to many cellular processes [2]. Anomalous zinc levels can cause serious problems. Zinc deficiency has been reported to cause chronic liver and kidney diseases while its surplus can cause neurotoxicity and dysregulation of calcium homeostasis [3–5]. Furthermore, zinc imbalance is directly related to diseases such as Alzheimer, Parkinson, amyotrophic lateral sclerosis, prostate cancer, diabetes, among others [6].

For this reason, Zn^{2+} detection has attracted increasing interest in the fields of chemistry and biology. Various methods for detecting and quantifying zinc ions have been devised, e.g., FAAS (Flame Atomic Absorption Spectrometry), electrochemical methods, and ICP (Inductively Coupled Plasma atomic emission spectrometry) [7]. However, these methods require time-consuming pre-treatment of samples by experienced professionals and costly equipment. In addition, detecting zinc ions is not a trivial task as metals belonging to the same group, which have similar chemical properties (e.g., cadmium), may interfere with its detection [8, 9].

Thus far, spectrofluorimetry has stood out as the most effective method for detecting Zn^{2+} ions in biological systems, given that the d^{10} electronic configuration of this ion makes it spectroscopically or magnetically silent [10]. In addition, the highly sensitive, selective, and non-destructive nature of fluorescence spectroscopy makes it a suitable technique for detecting metal ions in small quantities.

✉ Andréa Luzia Ferreira de Souza
andrealuziasouza@yahoo.com.br

[1] Universidade Federal do Rio de Janeiro, Campus Macaé Professor Aloísio Teixeira, CEP, Macaé, RJ 27930-560, Brazil

[2] Instituto de Macromoléculas, Universidade Federal do Rio de Janeiro, Cidade Universitária, CEP, Rio de Janeiro, RJ 21941-598, Brazil

[3] Pós-Graduação em Química (PGQu), Instituto de Química, Universidade Federal do Rio de Janeiro, Cidade Universitária, Rio de Janeiro, RJ CEP21941-909, Brazil

By means of fluorescence spectroscopy, metal ions can be detected by their forming luminescent coordination compounds [11]. This has considerably increased the importance of *N*-acylhydrazone compounds in the field of coordination chemistry because the nitrogen atom of the azomethine group (C=N) and the carbonyl oxygen (C=O) can act as complexation sites for metal ions. These complexation sites improve stability and enable the formation of a polydentate ligand [12].

This study aims at demonstrating the viability and effectiveness of employing the fluorescence properties of isoniazid-based *N*-acylhydrazones **HL1, HL2,** and **HL3** (**HL1–HL3)** varying their substituting groups (-H, -$N(CH_3)_2$, and -NO_2) to detect zinc ions. To this end, the selectivity and limit of detection (LOD) for Zn^{2+} ions in acetonitrile (ACN) medium were investigated. This study also examined the behavior of the ligands in question in the presence of Zn^{2+} and other metal ions by means of UV-vis and fluorescence techniques.

Experimental Section

The reagents isoniazid, benzaldehyde, 4-nitrobenzaldehyde, and 4-(*N*,*N*-dimethylamino)benzaldehyde (Sigma-Aldrich®) and glacial acid acetic (Vetec) were employed to synthesize **HL1–HL3**. Chloride salts of all cations (Sigma-Aldrich®) and HPLC-grade solvents (Tedia) were used without further purification.

The synthesis of *N*-acylhydrazone derivatives was carried out in an Anton Paar Monowave 300. UV-vis absorption spectra were recorded on a Shimadzu UV-2450 spectrophotometer and steady-state fluorescence spectra were recorded on an F9000 Edinburgh Instruments spectrofluorometer with a 450 W xenon arc lamp. TOF-EM analyses were performed by means of a high-resolution mass spectrometer (Q-TOF brand WATERS/MICROMASS model) with an 80–100 m/z scanner. ^{1}H NMR spectra were obtained on Bruker FT-400 MHz and FT-500 MHz spectrometers (USA) with DMSO-d_6 as solvent at the Farmanguinhos-FIOCRUZ (RJ) laboratory. Chemical shifts are reported in delta (δ) units relative to the singlet (0 ppm) of tetramethylsilane (TMS). Melting points of the derivatives were determined on a Fisatom melting-point apparatus.

Microwave Assisted-Synthesis of Isoniazid-Based N-Acylhydrazones Derivatives (HL1–HL3)

In a 30 mL vial, a mixture of isoniazid (3.0 mmol), aldehyde (3.0 mmol), and glacial acetic acid (~5 drops) in ethanol (15 mL) was stirred (1000 rpm) under microwave irradiation for 45 min at 140 °C [13]. After the reaction mixture was left to cool down to room temperature, the solid was filtered off and washed in cold ethanol. Then, the crude product was recrystallized in ethanol. The final products were characterized by melting point, quadrupole time-of-flight mass spectrometry (QTOF-EM), and ^{1}H NMR (Fig. S1–S6).

N′-Benzylidene isonicotinohydrazide (**HL1**): white solid; yield: 84%; mp: 189–190 °C; QTOF-EM found for $C_{13}H_{11}N_3O$ $(M + Na^+)$ $m/z = 248.079433$; ^{1}H NMR (400 MHz, DMSO-d_6) δ: 12.02 (s, 1H, NH); 8.48 (s, 1H, CH=N), 8.77 (d, 2H, J= 3.0 Hz, Ar-H), 7.82 (d, 2H, J= 6.0 Hz, Ar-H), 7.73 (d, 2H, J= 3.0 Hz, Ar-H), 7.45–7.16 (m, 3H, Ar-H).

N′-(4-*N*,*N*-Dimethylaminobenzylidene) isonicotinohydrazide (**HL2**): yellow solid, yield: 81%. mp: 203–205 °C. QTOF-EM found for $C_{14}H_{16}N_4O$ $(M + Na^+)$ $m/z = 291.121632$. ^{1}H NMR (500 MHz, DMSO-d_6) δ: 11.82 (s, 1H, NH), 8.78 (d, 2H, J= 5.0 Hz, Ar-H), 8.33 (s, 1H, CH=N), 7.83 (d, 2H, J= 5.0 Hz, Ar-H), 7.58 (d, 2H, J= 10.0 Hz, Ar-H), 6.78 (d, 2H, J= 10.0 Hz, Ar-H), 2.98 (s, 6H, N-CH_3).

N′-(4-Nitrobenzylidene) isonicotinohydrazide (**HL3**): yellow solid; yield: 92%; mp: 265–267 °C. QTOF-EM found for $C_{13}H_{10}N_4O_3$ $(M + Na^+)$ $m/z = 293.064511$ $(M + Na^+)$, ^{1}H NMR (400 MHz, DMSO-d_6) δ: 12.36 (s, 1H, NH), 8.82 (d, 2H, J= 6.0 Hz, Ar-H), 8.57 (s, 1H, CH=N), 8.33 (d, 2H, J= 8.7 Hz, Ar-H), 8.04 (d, 2H, J= 8.7 Hz, Ar-H), 7.85 (d, 2H, J= 6.0 Hz, Ar-H).

Measurement of Photophysical Properties of HL1–HL3

HL1–HL3 stock solutions were prepared in acetonitrile (ACN). Aqueous solutions of the metal salts under investigation were prepared with 100 equiv. of respective ligand. UV-vis spectra were obtained within the 200–500 nm range at room temperature, with solutions of 0.8 μmol.l^{-1}, 0.6 μmol.l^{-1}, and 1.6 μmol.l^{-1}, for **HL1–HL3**, respectively. Fluorescence assays were performed at room temperature, using SUPRASIL quartz cuvettes with 10 mm pathlength and transparent windows on all four sides. All the assays were performed after mixing for 5 min to ensure uniformity. Fluorescent spectra were recorded within the 400–680 nm range. The fluorescence of compounds **HL1–HL3** (0.8 μmol.l^{-1}, 0.6 μmol.l^{-1} and 1.6 μmol.l^{-1}, respectively) was evaluated in the presence of 100 equiv. of Zn^{2+} ions (λ_{ex} = 290 nm, 356 nm, and 322 nm for **HL1**, **HL2** and **HL3**, respectively).

As to titration, **HL2** concentration was kept constant (0.6 μmol.l^{-1}), while Zn^{2+} concentration varied from 0 to 160 equiv. (λ_{ex} = 356 nm, 400–680 nm). Limit of detection (LOD) and limit of quantification (LOQ) were estimated with the standard deviation of blank measurement. Selectivity assays were conducted at constant **HL2** concentration (0.6 μmol.l^{-1}), 100 equiv. of the metal ions under investigation (Na^+, Cd^{2+}, Zn^{2+}, Fe^{3+}, Mg^{2+}, Ca^{2+}, and Cu^{2+}), and

Scheme 1 Synthetic route to obtain *N*-acylhydrazones derivatives HL1–HL3

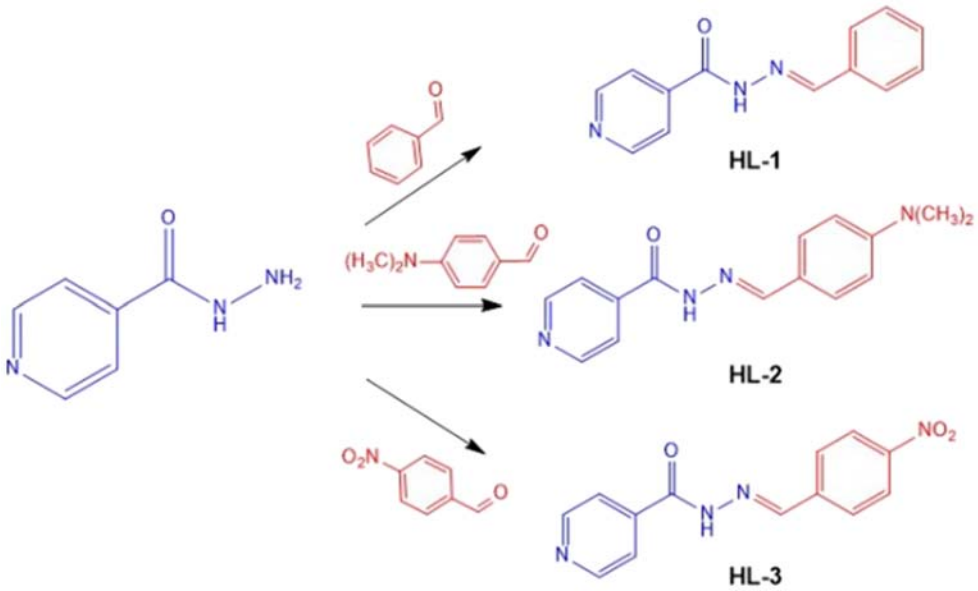

ligand concentration equal to 0.6 μmol.l^{-1}. The solutions were prepared with ACN at 25 °C, λ_{ex} = 356 nm, and within the 400–680 nm range.

Job's Plot was performed in a front-face fluorometer with concentrations of **HL2** and Zn^{2+} ions varying from 0 to 20 μmol.l^{-1} in ACN, at 25 °C, λ_{ex} = 356 nm, and 379–700 nm scan.

Calculations of Binding Constants and LOD

The binding constant for **HL2** was determined by means of fluorescence titration and by plotting a graph of F_{max} vs. [M] μmol.l^{-1}. Limit of detection (LOD) and limit of quantification (LOQ) of **HL2** for Zn^{2+} ions in ACN were measured with the help of blank standard method (LOD = 3σ/*m*; LOQ = 10σ/*m*)

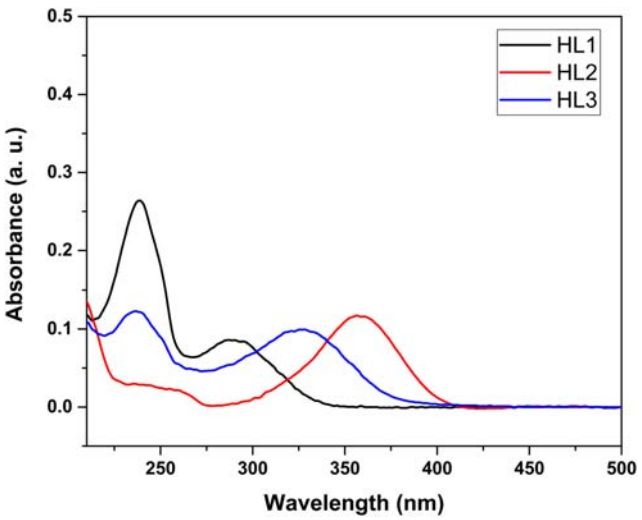

Fig. 1 UV–vis absorption spectra for HL1–HL3 (0.8 μmol.l^{-1}, 0.6 μmol.l^{-1} and 1.6 μmol.l^{-1}, respectively) in ACN at 25 °C

and estimated from linear relationships between maximum emission intensity at 579 nm and Zn^{2+} concentration.

Aggregation

Front-face fluorometry was also used for the aggregation assay, in which **HL2** concentration varied from 5.0–500 μmol.l^{-1} with concentration of Zn^{2+} ions at 100 equiv. of **HL2**, scan within the 380–680 nm range, and λ_{ex} at 360 nm.

Strip Test

Strip tests were conducted in two steps. First, 3 × 1 cm filter paper strips were immersed in an **HL2**-ACN solution (1 × 10^{-5} mol.l^{-1}). After drying, the strips were immersed in aqueous zinc chloride solution at different concentrations (from 1 × 10^{-3} to 1 × 10^{-2} mol.l^{-1}). Fluorescence responses of the strips were analyzed under 365 nm UV-irradiation.

Results and Discussion

The isoniazid-based *N*-acylhydrazone derivatives **HL1–HL3** were synthesized by the Schiff Base condensation reaction as described in our previous study (outlined in Scheme 1) [13]. Microwave-assisted reactions of isoniazid with respective aldehyde (benzaldehyde, 4-(*N*,*N*-dimethylamino)benzaldehyde, and 4-nitrobenzaldehyde dissolved in ethanol), for 45 min, at 140 °C yielded white (**HL1**) and yellow (**HL2** and **HL3**) solids. Then, these solids were recrystallized in ethanol. ^{1}H NMR results and quadrupole time-of-flight mass spectrometry

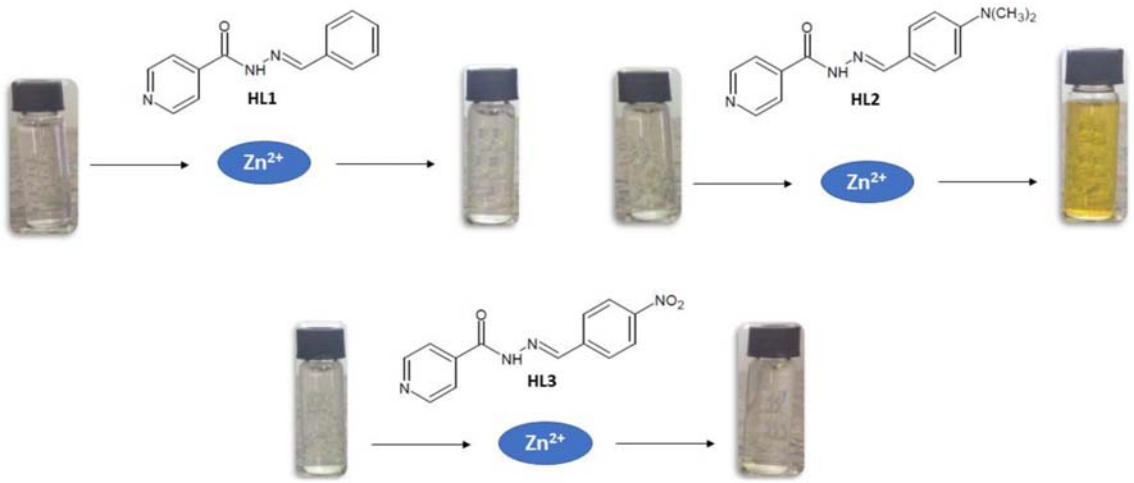

Fig. 2 Qualitative colorimetric effect of HL1–HL3 with Zn^{2+} ions in ACN at 25 °C

(QTOF-EM) spectra of these recrystallized solids are shown in the supporting information section below (Fig. S1–S6).

Colorimetric Sensing of HL1-HL3

The absorption spectra of free **HL1–HL3** in dilute ACN solutions (abs. ~ 0.2) is characterized by two main absorption bands in the 200–500 nm region as shown in Fig. 1. The bands at higher energy are ascribed to $\pi \rightarrow \pi^*$ transitions ($\varepsilon_{\mathbf{HL1}} = 3.29 \times 10^5$, $\varepsilon_{\mathbf{HL2}} = 4.99 \times 10^4$, and $\varepsilon_{\mathbf{HL3}} = 7.6 \times 10^4$ L mol^{-1} cm^{-1}) in the aromatic system of the compounds while the low intensity bands at lower energy are attributed to $\pi \rightarrow \pi^*$ transitions ($\varepsilon_{\mathbf{HL1}} = 1.07 \times 10^5$, $\varepsilon_{\mathbf{HL2}} = 1.94 \times 10^5$, and $\varepsilon_{\mathbf{HL3}} = 6.2 \times 10^4$ L mol^{-1} cm^{-1}) of C=N and C=O groups [14].

The addition of a solution of Zn^{2+} ions to **HL2** leads to its color changing from colorless to strong yellow (Fig. 2). Since **HL1** and **HL3** showed no changes in absorption spectra in the presence of Zn^{2+}, only the absorption spectrum of **HL2** will be presented here. The ligands **HL1** and **HL3** did not change color when in contact with Zn^{2+} ions in ACN (Fig. 2), either.

The behavior of *N*-acylhydrazone **HL2** in the presence of Cd^{2+}, Cu^{2+}, Fe^{3+} ions was also investigated and compared to that in the presence of Zn^{2+} ions in ACN. In the assays with metal ions, their presence frequently caused **HL2** to exhibit non-significant changes (Fig. S7). However, in the case of Cd^{2+}, Cu^{2+}, Fe^{3+}, and Zn^{2+} ions, a distinctive absorption shift was observed, as shown in Fig. 3. UV–vis absorption spectra of acylhydrazone **HL2** in the presence of different metal ions is shown in Fig. S8.

As to **HL2** in the presence of Zn^{2+} ions, absorbance bands at 259 nm and 356 nm shifted to 240 nm and 364 nm, respectively. These changes show that adding Zn^{2+} enlarged the conjugated system of the ligand, implying that the nitrogen atom of the C=N group and the oxygen atom of the C=O group of the ligand have successfully coordinated to the central Zn^{2+} ion [14–16]. For **HL2** in the presence of Cu^{2+} ions,

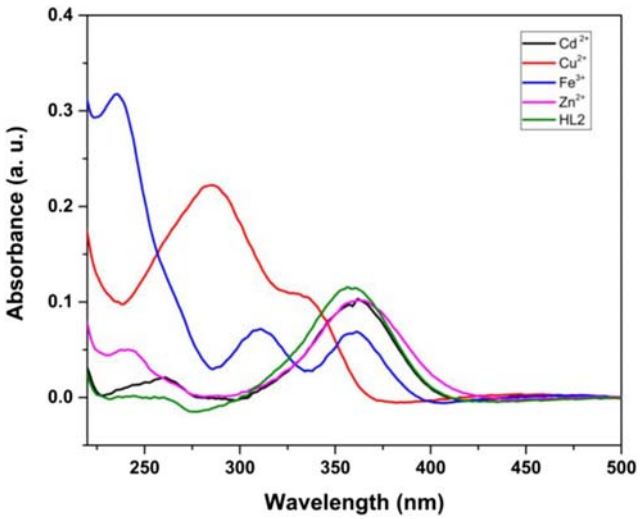

Fig. 3 UV–vis absorption spectra of acylhydrazone HL2 in the presence of different metal ions (1 equiv.) in ACN at 25 °C

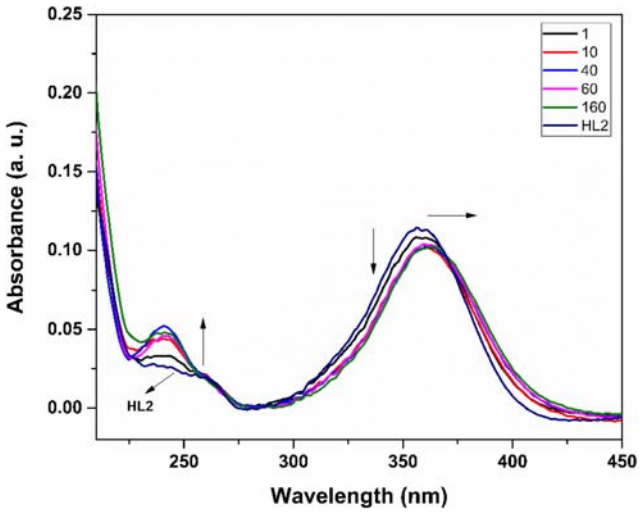

Fig. 4 UV-vis titration spectra for HL2 (0.6 μmol.l^{-1}) from 0 to 160 equiv. of Zn^{2+} ions

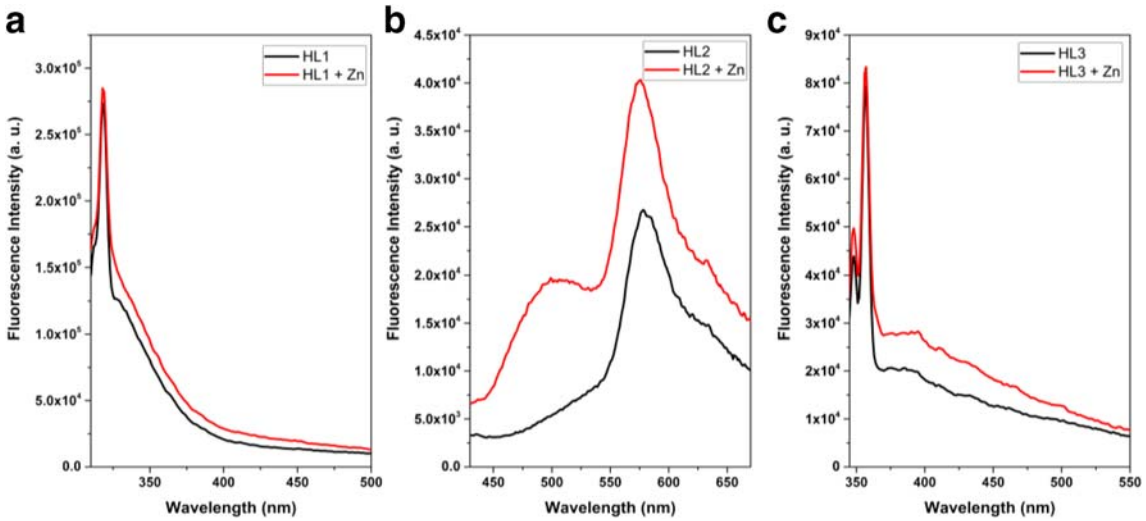

Fig. 5 100 equiv. Zn^{2+}: (A) **HL1** $\lambda_{ex} = 290$ nm, $\lambda_{em} = 310–550$ nm; (B) **HL2** $\lambda_{ex} = 356$ nm, $\lambda_{em} = 400–680$ nm; (C) **HL3** $\lambda_{ex} = 322$ nm, $\lambda_{em} = 342–550$ nm

the *N*-acylhydrazone-related band shifted to a higher energy region (332 nm). In addition, it is possible to observe a very intense band at 285 nm, associated to the formation of another entity [17, 18]. There are reports in the literature of 1,3,4-oxadiazoles deriving from the oxidation of *N*-acylhydrazones with Cu^{2+} as catalyst [19]. Concerning **HL2** + Fe^{3+} ions, electronic spectra show a blue shift, implying coordination with **HL2**. The band at 359 nm can be attributed to $n \rightarrow \pi^*$ transitions for the azomethine groups whereas the ones at 310 nm and 238 nm are associated to ligand-metal interaction and $\pi \rightarrow \pi^*$ transitions of ethereal oxygen of the ligands, respectively. No *d-d* transitions were observed from 600 nm to 800 nm [20].

These changes are related to interactions between metal ions and ligand. A bathochromic shift (8 nm) of the band at 356 nm occurred for **HL2** in the presence of Zn^{2+} ions, which is attributed to the metal complex structure becoming more rigid (CHEF-chelation enhanced fluorescence mechanism). Moreover, the intensity of this band decreased, prompting the solution color to change from colorless to yellow (Fig. S7), as the absorbance peaks of the **HL2** + Zn^{2+} complex shifted to the visible region. This color change, selective for Zn^{2+} ions, was observed through the naked eye, thereby making **HL2** a promising naked-eye Zn^{2+} colorimetric sensor. It is important to note that the intense yellow color exhibited by the **HL2** + Fe^{3+} complex in Fig. S7 most likely results from the color of the aqueous $FeCl_3$ salt solution itself (Fig. S7).

The sensitivity of the chemosensor **HL2** to Zn^{2+} ions was investigated by measuring absorbance at varying Zn^{2+} concentrations (0–100 equiv.) (Figure S9). The absorbance band at 242 nm gradually increased, and the band at 356 nm shifted to 362 nm (Fig. 4), implying the formation of an **HL2** + Zn^{2+} complex.

Fluorescence Sensing of N-Acylhydrazones HL1–HL3

Free **HL1** and **HL3** did not exhibit fluorescence when excited at 290 nm and 332 nm, respectively (Fig. 5). When excited at 356 nm, **HL2** exhibited an almost imperceptible fluorescence emission band at 591 nm. However, a significant change in fluorescence spectra occurred upon addition of Zn^{2+} ions: a band appeared at 500 nm while the band at 582 nm increased. This fluorescence switch "*off–on*" phenomenon can be explained via photoinduced electron transfer (PET) mechanism.

HL2 fluorescence can be attributed to the stability of the complex formed. The $N(CH_3)_2$ group increases the electronic density of the azomethine group making it a better active site for coordination with Zn^{2+} (Fig. 6). In addition, NO_2 groups

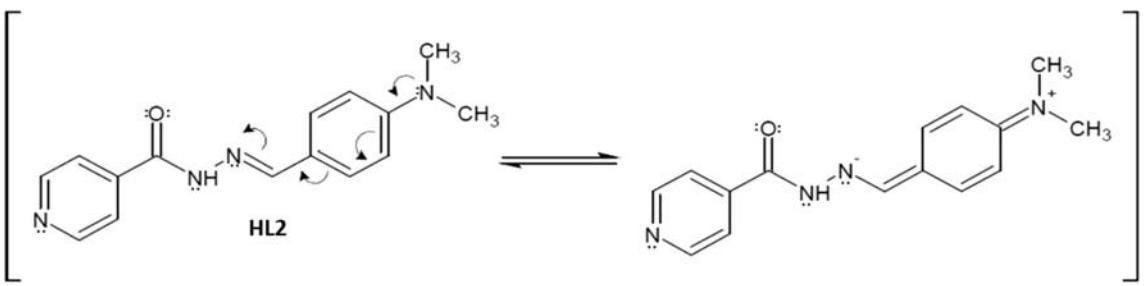

Fig. 6 Resonance structures of HL2 [22]

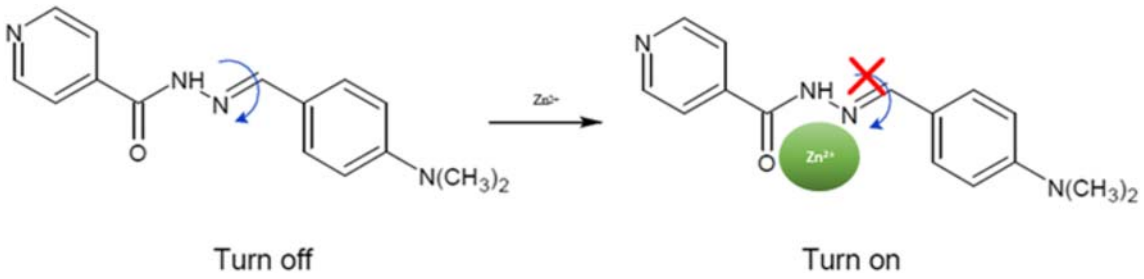

Fig. 7 Inhibition of isomerization by adding Zn^{2+} ion [23]

tend to give rise to quenching due to S1 → S0 internal conversion and intersystem crossing involving electron-withdrawing of NO_2 groups. In contrast, the lone pair of amino group can increase n → π* transition, leading to stronger fluorescence emission [21].

In the case of *N*-acylhydrazones, coordination with the Zn^{2+} ion is decisive for luminescence to occur, since coordination with the metal ion can inhibit C=N bond isomerization, thereby reducing energy loss from non-radiative processes. The coordinating compound formed can also prevent a PET-type process from occurring, in which free electrons of azomethine nitrogen, once coordinated with the metal ion, cannot be transferred to the HOMO orbital of the fluorophore, triggering a CHEF-type process (Fig. 7) [23, 24].

Fluorescence Titration

The sensibility of the chemosensor was investigated via titration with **HL2** and different concentrations of Zn^{2+} ions. As concentration of Zn^{2+} ions gradually increased, fluorescent emission intensified at 503 nm and 579 nm, with a linear response $R^2 = 0.9878$, (Fig. 8a). Linear adjustment was performed up to the limit of linearity of the curve plotted from the experimental data.

LOD and LOQ values for **HL2** are 0.43 and 0.93 μmol.l^{-1} ($R^2 = 0.9878$), respectively, where σ is the standard deviation of the blank measurements, and *m* is the slope of the intensity vs. sample concentration curve (Fig. 8b). The LOD value for **HL2** was lower than 76 μmol.l^{-1}, the maximum acceptable concentration of Zn^{2+} ions in drinking water established by the World Health Organization (WHO), indicating that this derivative can be an effective Zn^{2+} ion sensor in aqueous solutions [25].

Binding interactions between **HL2** and Zn^{2+} ions were estimated by means of equilibrium equations (Eqs. 1 and 2).

$$L + M \leftrightarrow LM \therefore K_1 = \frac{[LM]}{[M][L]} \tag{1}$$

$$LM + L \leftrightarrow L_2M \therefore K_2 = \frac{[L_2M]}{[LM][L]} \tag{2}$$

The graph plotted using the Benesi-Hildebrand method did not provide a linear relationship, implying that the compound formed in solution has a coordination system different from 1:1. For this reason, the F vs. [M] graph was not linearized to obtain more reliable results [26]. Once mass balances for [L] and [M] were performed and replaced in Eqs. 1 and 2, it was

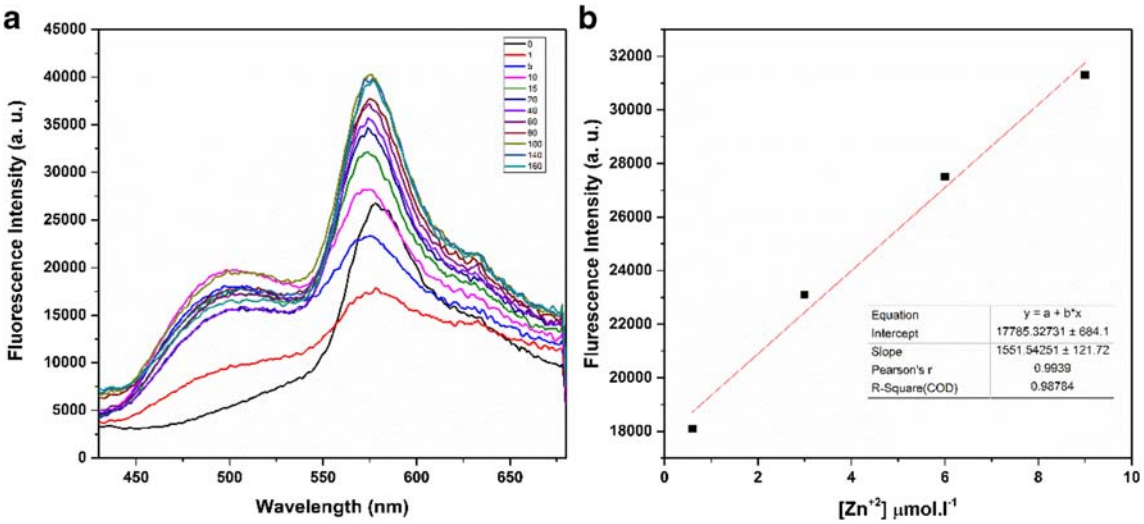

Fig. 8 (**a**) Fluorescence titration emission spectra of **HL2** (0.6 μmol.l^{-1}) upon addition of Zn^{2+} ions (0.0–160 equiv.). (**b**) LOD [Zn] = 0–9 μmol.l^{-1} with an excitation at 356 nm; $\lambda_{em} = 579$ nm

possible to estimate the constants K_1 and K_2 in Eq. 3, which describes the F vs. [M] curve [27].

$$Ax^3 + Bx^2 + Cx + D = 0 \quad (3)$$

Where A is (K_1K_2), B is $(K_1 + (K_1K_2)2[L_0]–[M_0])$, C is $(1 + K_1(L_0] + [M_0])$ and D is $–[M_0]$.

The value obtained for K_1 and K_2 were 9.5×10^4 l.mol^{-1} and 5.04×10^{12} l.mol^{-1}, respectively. K_2 is a much larger value than K_1, which indicates a greater tendency for the 2:1 (ligand:metal) coordination compound to form. In addition, the high K_2 value also indicates strong interaction of Zn^{2+} ion with the ligand, giving rise to more stable complexes. Figure 9 shows two points around which the 1:1 complex and 2:1 complex are formed in solution: 24 μmol.l^{-1} and 60 μmol.l^{-1}. Afterwards, fluorescence intensity stabilizes even as Zn^{2+} ion concentration increases in the medium.

Competitive Metal Ion Titrations

Despite changes in the UV-vis spectra of **HL2** in the presence of Fe^{3+} and Cu^{2+} ions as compared to the spectrum of the compound **HL2** + Zn^{2+}, fluorescence assays show that **HL2** has a comparatively higher emission intensity, i.e., greater selectivity to Zn^{2+} ion. We also observed that adding the metal ion Fe^{3+} suppressed the emission of **HL2**, as shown in Fig. 10. Finally, in spite of the **HL2** solution changing color slightly upon addition of Cd^{2+} ions, we did not observe fluorescence in the **HL2** + Cd^{2+} compound.

Given that selectivity is an important parameter for optical sensors, the interference caused by Cd^{2+} ions was investigated due to their chemical proprieties being similar to those of Zn^{2+} ions [28–31]. Figure 11 shows that the metal ion Cd^{2+}, a common competitor for sensors responding to Zn^{2+} ions, did not significantly interfere with Zn^{2+} detection using **HL2** in ACN.

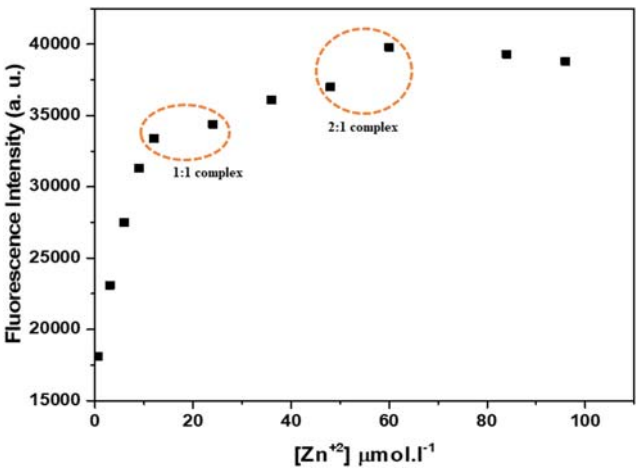

Fig. 9 Fluorescence titration emission spectra for HL2 (0.6 μmol.l^{-1}) upon addition of Zn^{2+} ions (0.0–160 equiv.), $\lambda_{ex} = 356$ nm, emission fixed at 579 nm

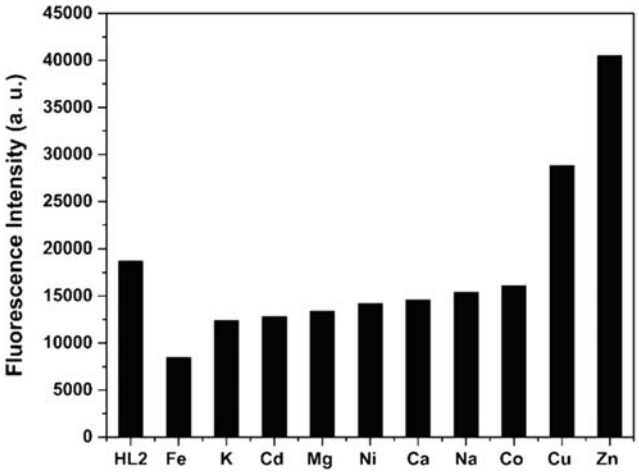

Fig. 10 Fluorescent intensity for **HL2** (0.6 μmol.l^{-1}) after treatment with 60 μmol.l^{-1} (100 equiv.) of metal ions: Fe^{3+}, K^+, Cd^{2+}, Mg^{2+}, Ni^{2+}, Ca^{2+}, Na^+, Co^{2+}, Cu^{2+}, and Zn^{2+} in ACN, $\lambda_{em} = 579$ nm

Figure 11 shows that the ligand-related band at 579 nm in the spectrum represented by a black line broadened and decreased in intensity upon addition of Cd^{2+} ions due to their coordinating with free **HL2** in the medium. On the other hand, in the same spectrum, the intensity of the band at 503 nm intensified due to formation of compounds coordinated with Zn^{2+} ions (**HL2** + Zn^{2+}). This suggests that Cd^{2+} ions do not interfere with **HL2** coordinating with Zn^{2+} ions. This behavior may be attributed to Cd^{2+} having a greater atomic radius, which generates higher steric impediment to the formation of coordinated compounds. Besides, Zn^{2+} is a stronger Lewis acid than Cd^{2+}, which favors interaction with the active fluorophore sites [32].

Table 1 shows comparable results for some of the previously mentioned sensors. **HL2** exhibits the highest binding constant, which indicates that this ligand can promote strong interactions with Zn^{2+} ions even at low concentrations. Moreover, LOD values for HL2 are of the same order of

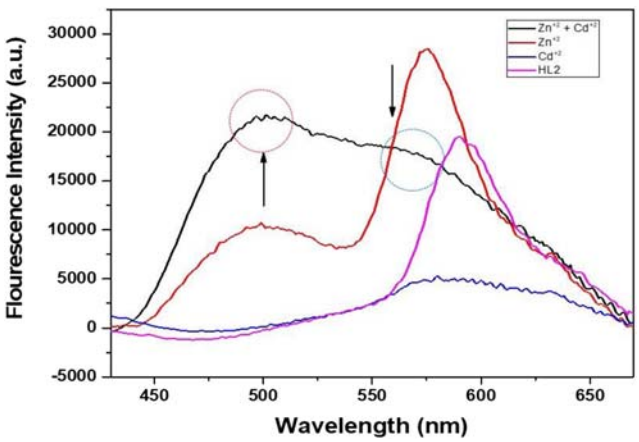

Fig. 11 Competitive selectivity of **HL2** (0.6 μmol l^{-1}) towards Cd^{2+} and Zn^{2+} ions (100 equiv.) ($\lambda_{ex} = 356$ nm)

Table 1 Binding constant and LOD values for *N*-acylhydrazone derivatives as 'turn on' fluorescent sensors for zinc ions [33–36]

Entry	Ligand Structure	Stoichiometry	Binding Constant ($l.mol^{-1}$)	LOD ($\mu mol.l^{-1}$)	Ref.
1	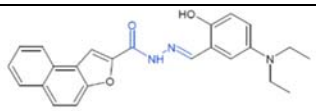	1:1	4.69×10^{6}	0.13	[33]
2	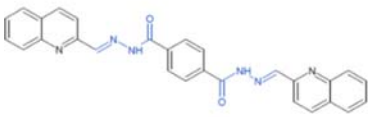	2:1	$8.14\times10^{5*}$	0.073	[34]
3	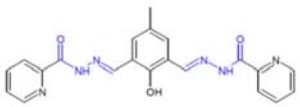	1:2	5.58×10^{5}	0.23	[35]
4	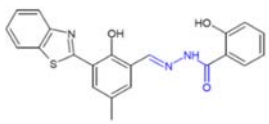	1:1	3.19×10^{4}	0.127	[36]
5	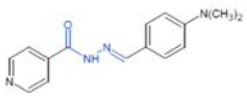	2:1	$5.04\times10^{12*}$	0.43	This study

* Binding Constant for K_2.

magnitude as those values for the acylhydrazone derivatives in Table 1.

Stoichiometry of Sensing Probe with Metal Ions

The stoichiometry of the metal complex formed by **HL2** and Zn^{2+} was determined by *Job's Plot* titration method (Fig. 12).

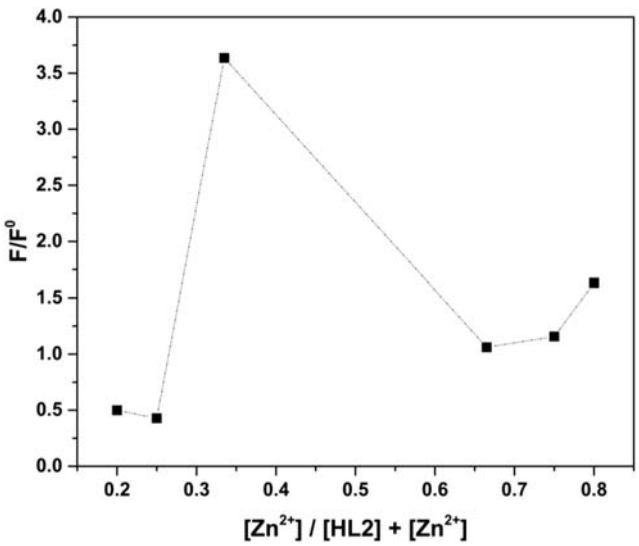

Fig. 12 *Job's Plot* titration for **HL2** + Zn^{2+} [sol.] = 20 $\mu mol.l^{-1}$, indicating 2:1 stoichiometry at λ_{max} = 579 nm

Fluorescent intensity peaked at 0.35 M ratio, indicating a 2:1 stoichiometric binding interaction between **HL2** and Zn^{2+}.

Compounds with aromatic and well-conjugated structures are known for displaying π-π stacking aggregation, which in turn can suppress luminescence, making their use in optoelectronic devices more difficult [37–39]. Therefore, it is important to evaluate aggregation in the present system (**HL2** + 100

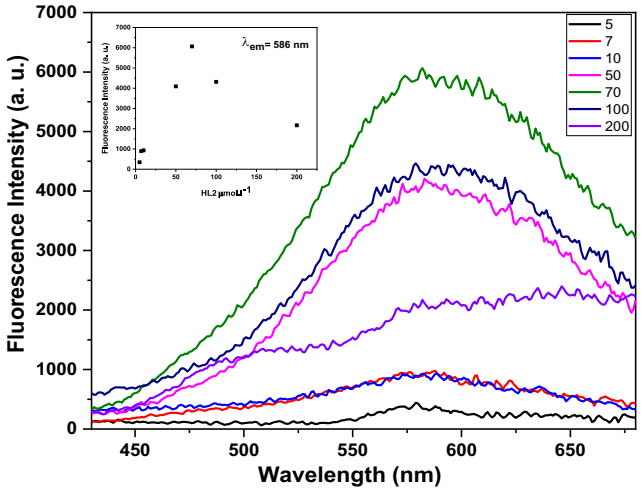

Fig. 13 The fluorescence intensity curves at different concentrations of **HL2** (5.0–500 $\mu mol.l^{-1}$) in the presence of 100 equiv. Zn^{2+} ions, in ACN at 25 °C, λ_{ex} = 360 nm

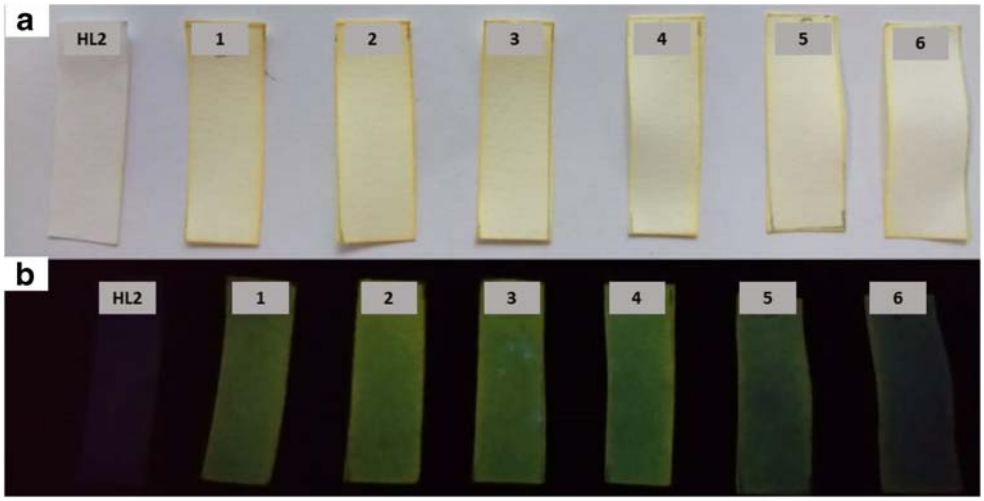

Fig. 14 Strips test after immersion in **HL2** (1×10^{-5} mol.l^{-1}) and $ZnCl_2$ solution: 1–1×10^{-2} mol.l^{-1}; 2–9×10^{-3} mol.l^{-1}; 3–7×10^{-3} mol.l^{-1}; 4–5×10^{-3} mol.l^{-1}; 5–3×10^{-3} mol.l^{-1}; 6–1×10^{-3} mol.l^{-1}: (**a**) natural light irradiation; (**b**) 365 nm UV lamp irradiation

equiv. of Zn^{2+} ions), as shown in Fig. 13. The results show that at **HL2** concentrations higher than 70 μmol.l^{-1}, fluorescence intensity decreases significantly, possibly due to the beginning of the aggregation process. In this direction, it is important to note that the results presented so far in this study have not been affected by aggregation.

Strips Test

Test results indicated that it was possible to detect the presence of Zn^{2+} by immersing strips in a ligand solution at 1×10^{-5} mol.l^{-1} concentration. Figure 14(a) shows a slight color change to yellow after immersing the strips in the $ZnCl_2$ solution. The strips exhibited fluorescence under UV 365 nm irradiation (Fig. 14(b)), which intensified as $ZnCl_2$ concentration increased, indicating that the derivative **HL2** is capable of detecting Zn^{2+} ions by means of a simple and practical method. In addition, the reversibility assay was conducted for the ligand. Fluorescence was observed upon adding 5 equiv. of Zn^{2+} to a methanolic solution of **HL2** (15 μmol.l^{-1}). However, adding 10 equiv. of EDTA to the same solution led to rapid color change and fluorescence suppression, implying reversibility of **HL2**, which may thus be reused to detect the presence of Zn^{2+} ions multiple times [40–43].

Conclusion

The simple isoniazid-based *N*-acylhydrazone derivative **HL2** exhibited higher fluorescence intensity as compared to that of **HL1** and **HL3**. This higher fluorescence intensity is attributed to the influence of the aryl-substituted donor group in coordination with Zn^{2+} ions forming more stable complexes. Coordination inhibited isomerization characteristic of *N*-acylhydrazones, leading to a CHEF-type emission process. The LOD and LOQ values, 0.43 μmol.l^{-1} and 0.93 μmol.l^{-1}, respectively, indicate that **HL2** is sensitive and selective to Zn^{2+} ions. Results also show that the **HL2** + Zn^{2+} complex is highly stable (as corroborated by the binding constant value of 5.04×10^{12} l.mol^{-1}) and selective for Zn^{2+} ions even in the presence of Cd^{2+} and other metal ions. Furthermore, the *Job's Plot* performed indicated the formation of a complex with 2:1 stoichiometry (**HL2**:Zn^{2+}). The strips test with **HL2** in aqueous solutions of varying Zn^{2+} concentrations showed fluorescence under UV lamp irradiation at 365 nm. Altogether, these results demonstrate the viability and effectiveness of using the *N*-acylhydrazone derivative **HL2** as a chemosensor selective for Zn^{2+} ions.

Supplementary Information The online version contains supplementary material available at https://doi.org/10.1007/s10895-020-02651-7.

Acknowledgments The authors would like to thank Farmanguinhos-FIOCRUZ for the QTOF-EM and ^{1}H NMR spectra data.

References

1. Vallee BL, Falchuk KH (1993) The biochemical basis of zinc physiology. Physiol Rev 73:79–118
2. Buccella D, Horowitz JA, Lippard SJ (2011) Understanding zinc quantification with existing and advanced ditopic fluorescent zinpyr sensors. J Am Chem Soc 133:4101–4114
3. Frederickson CJ, Koh JY, Bush AI (2005) The neurobiology of zinc in health and disease. Nat Rev Neurosci 6:449–462
4. Jurowski K, Szewczyk B, Nowak G, Piekoszewski W (2014) Biological consequences of zinc deficiency in the pathomechanisms of selected diseases. J Biol Inorg Chem 19: 1069–1079
5. Takeda A (2014) Significance of Zn2+ signaling in cognition: insight from synaptic Zn2+ dyshomeostasis. J Trace Elem Med Biol 28:393–396
6. Chasapis CT, Spiliopoulou CA, Loutsidou AC, Stefanidou ME (2012) Zinc and human health: an update. Arch Toxicol 86:521–534
7. Chae JB, Lee H, Kim C (2020) Determination of zinc ion by a Quinoline-based fluorescence Chemosensor. J Fluoresc 30:347–356

8. Ding A, Tang F, Wang T et al (2015) A α-cyanostilbene-modified Schiff base as efficient turn-on fluorescent chemosensor for Zn2+. J Chem Sci 127:375–382
9. Dong Y, Fan R, Chen W, Wang P, Yang Y (2017) A simple quinolone Schiff-base containing CHEF based fluorescence "turn-on" chemosensor for distinguishing Zn2+ and Hg2+ with high sensitivity, selectivity and reversibility. Dalt Trans 46:6769–6775
10. Li P, Zhou X, Huang R, Yang L, Tang X, Dou W, Zhao Q, Liu W (2014) A highly fluorescent chemosensor for Zn2+ and the recognition research on distinguishing Zn2+ from Cd2+. Dalt Trans 43: 706–713
11. Sharma S, Pradeep CP, Dhir A (2016) Benzimidazole based 'turn on' fluorescent Chemodosimeter for zinc ions in mixed aqueous medium. J Fluoresc 26:1439–1445
12. Manikandan R, Viswanathamurthi P, Muthukumar M (2011) Ruthenium(II) hydrazone Schiff base complexes: synthesis, spectral study and catalytic applications. Spectrochim Acta - Part A Mol Biomol Spectrosc 83:297–303
13. Santos DC, Henriques RR, Lopes MAA Jr et al (2020) Acylhydrazones as isoniazid derivatives with multi-target profiles for the treatment of Alzheimer's disease: radical scavenging, myeloperoxidase/acetylcholinesterase inhibition and biometal chelation. Bioorg Med Chem 28:115470
14. Pérez-Rebolledo A, Piro OE, Castellano EE, Teixeira LR, Batista AA, Beraldo H (2006) Metal complexes of 2-benzoylpyridine semicarbazone: spectral, electrochemical and structural studies. J Mol Struct 794:18–23
15. Gili P, Palacios MS, Islands C, Lahoz FV (1992) Complexes of copper (II) and nickel (II) with the new ligand N-[2-(3-ethyl-Indole)]Pyridoxaldimine. X-ray crystal structure of Bis{N-[2(3-ethyl-Indole)]Pyridoxaldiminate}nickel (II). Polyhedron 2:2171–2178
16. Raman N, Ravichandran S, Thangaraja C (2004) Copper(II), cobalt(II), nickel(II) and zinc(II) complexes of Schiff base derived from benzil-2,4-dinitrophenylhydrazone with aniline. J Chem Sci 116:215–219
17. Li AF, He H, Ruan Y Bin, et al (2009) Oxidative cyclization of N-acylhydrazones. Development of highly selective turn-on fluorescent chemodosimeters for Cu2+. Org Biomol Chem 7:193–200
18. Xiang Y, Tong A (2008) Ratiometric and selective fluorescent chemodosimeter for cu(II) by cu(II)-induced oxidation. Luminescence 23:28–31
19. Nan Q, Rong P, Jiang Y, Yang R (2017) New highly selective turn-on fluorescence receptor for the detection of copper(II). Spectrochim Acta - Part A Mol Biomol Spectrosc 174:307–315
20. Zhu W, Yang L, Fang M, Wu Z, Zhang Q, Yin F, Huang Q, Li C (2015) New carbazole-based Schiff base: colorimetric chemosensor for Fe3+ and fluorescent turn-on chemosensor for Fe3+ and Cr3+. J Lumin 158:38–43
21. Valeur B, Berberan-Santos MN (2012) Molecular fluorescence: principles and applications. Wiley-VCH Verlag GmbH & Co. KGaA, Weinheim
22. De Albuquerque MA, Goulart CM, De Amorim APO et al (2013) Novas formulações de tiossemicarbazonas e extrato vegetal de Talinum triangulare com potencial atividade anticorrosão. Rev Virtual Quim 5:734–745
23. Wu J, Liu W, Ge J, Zhang H, Wang P (2011) New sensing mechanisms for design of fluorescent chemosensors emerging in recent years. Chem Soc Rev 40:3483–3495
24. Formica M, Fusi V, Giorgi L, Micheloni M (2012) New fluorescent chemosensors for metal ions in solution. Coord Chem Rev 256: 170–192
25. Kumari B, Lohar S, Ghosh M, Ta S, Sengupta A, Banerjee PP, Chattopadhyay A, Das D (2016) Structurally characterized Zn2+ selective Ratiometric fluorescence probe in 100% water for HeLa cell imaging: experimental and computational studies. J Fluoresc 26:87–103
26. Thordarson P (2011) Determining association constants from titration experiments in supramolecular chemistry. Chem Soc Rev 40: 1305–1323
27. Hargrove AE, Zhong Z, Sessler JL, Anslyn EV (2011) Algorithms for the determination of binding constants and enantiomeric excess in complex host: guest equilibria using optical measurements. New J Chem 34:348–354
28. Wang JH, Liu YM, Chao J Bin, et al (2020) A simple but efficient fluorescent sensor for ratiometric sensing of Cd2+ and bio-imaging studies. Sens Actuators B Chem 303:127216
29. Wang P, Wu X, Wu J, Liao Y (2019) Highly selective and sensitive peptide-based fluorescent chemosensor for detection of zinc(II) ions in aqueous medium and living cells. J Photochem Photobiol A Chem 382:111929
30. Lu ZN, Wang L, Zhang X, Zhu ZJ (2019) A selective fluorescent chemosensor for Cd2+ based on 8-hydroxylquinoline-benzothiazole conjugate and imaging application. Spectrochim Acta - Part A Mol Biomol Spectrosc 213:57–63
31. Hariharan PS, Anthony SP (2014) Selective turn-on fluorescence for Zn(2+) and Zn(2+)+cd(2+) metal ions by single Schiff base chemosensor. Anal Chim Acta 848:74–79
32. Zhu L, Yuan Z, Simmons JT, Sreenath K (2015) Zn(II)-coordination modulated ligand pohotophysical processes - the development of fluorescent indicators for imaging biological Zn(II) ions. RSC Adv 4:20398–20440
33. Guan J, Zhang P, Wei TB, Lin Q, Yao H, Zhang YM (2014) A highly selective PET-based chemosensor for instant detecting of Zn2+. RSC Adv 4:35797–35802
34. Cho HJ, Kim T, Kim H, Song C (2020) Solid-state emissive Metallo-Supramolecular assemblies of Quinoline-based acyl Hydrazone. Sensors 20:1–12
35. Datta BK, Thiyagarajan D, Samanta S, Ramesh A, Das G (2014) A novel chemosensor with visible light excitability for sensing Zn2+ in physiological medium and in HeLa cells. Org Biomol Chem 12:4975–4982
36. Liu TT, Xu J, Liu C guo, et al (2020) A novel dual-function probe for recognition and differentiation of Zn2+ and Al3+ and its application. J Mol Liq 300:112250
37. Maia PJS, De Aguiar I et al (2018) Chemistry singlet oxygen production by a polypyridine ruthenium (II) complex with a perylene monoimide derivative: a strategy for photodynamic inactivation of Candida albicans. J Photochem Photobiol A Chem 353:536–545
38. Maia PJS, Ferreira J et al (2019) Photophysical properties of a perylene derivative for use as catalyst in ethanol eletrooxidation. Res Chem Intermed 45:5451–5472
39. Maia JPS, Medeiros E et al (2018) Synthesis and characterization of a perylene derivative and its application as catalyst for ethanol electro-oxidation. Chem Pap 72:1021–1030
40. Dong W, Akogun SF, Zhang Y et al (2017) Reversible " turn-on " fluorescent sensor for selective detection of. Sensors Actuators B Chem 238:723–734
41. Gupta VK, Singh AK, Kumawat LK (2014) Thiazole Schiff base turn-on fluorescent chemosensor for Al3+ ion. Sens Actuators B Chem 195:98–108
42. Gupta VK, Singh AK, Kumawat LK (2014) A turn-on fluorescent Chemosensor for Zn2+ ions based on Antipyrine schiff base. Sens Actuators B Chem 204:507–5014
43. Jiménez-sánchez A, Farfán N, Santillan R (2013) A reversible fluorescent–colorimetric Schiff base sensor for Hg2+ ion. Tetrahedron Lett 54:5279–5283